Trends in Microbiology

CellPress
REVIEWS

Review

RTX Adhesins are Key Bacterial Surface Megaproteins in the Formation of Biofilms

Shuaiqi Guo,[1] Tyler D.R. Vance,[2] Corey A. Stevens,[2] Ilja Voets,[1] and Peter L. Davies[2,*]

Gram-negative bacteria produce repeats-in-toxin adhesion proteins (RTX adhesins) to facilitate microbial adhesion. These large, multidomain proteins share a common architecture comprised of four regions. First to emerge from the bacterium, C terminal end leading, is the RTX export sequence that directs the protein through the type 1 secretion system (T1SS). This is followed by the ligand-binding region responsible for host adhesion and cohesion, which contains diverse ligand-binding domains. These serve a zip code function to direct bacteria to a particular environmental niche. Thereafter is a large extension region consisting of tens to hundreds of tandem bacterial immunoglobulin-like (Big) domains, whose function is to extend the reach of the ligand-binding domains away from the bacterial surface. Lastly, there is a conserved N terminal cell-membrane-anchor region that retains the adhesin within the secretion system. This is also a site of *in situ* proteolysis, when nutrients are scarce, that enables the bacterium to leave the biofilm. In this review, the four regions of RTX adhesins are presented in the order in which they emerge from the cell during synthesis and retention.

Highlights

RTX adhesins are megaproteins displayed on the bacterial surface via passage through the type 1 secretion system.

At the distal end of these long adhesins are ligand-binding domains of different types that determine the substrates and partners to which the bacteria bind when forming biofilms.

Knowledge about these binding domains and their ligands could be used to weaken, enhance, or alter biofilm formation.

At the proximal end of the RTX adhesins are domains that can retain the protein in the outer membrane with a built-in proteolytic release mechanism.

Secretion of Adhesins and Retention in the Outer Membrane

Bacteria have evolved many different methods for the export of proteins into the extracellular space. While Gram-positive bacteria can use the Sec and Tat pathways to pass proteins through their single-layered membrane, Gram-negative bacteria are presented with the extra hurdle of a dual membrane, necessitating the evolution of a series of complex systems (types 1 to 6) [1]. Aside from simple secretion, many of these systems are also able to localize proteins – such as adhesins – to the surface of the outer membrane. For most nonfimbrial adhesins (or adhesins made up of a single polypeptide chain) this localization is achieved via one of two methods [2]. The first is the type 5 secretion system (T5SS), which uses a C terminal autotransporter domain as a channel that self-inserts into the outer membrane and facilitates the threading of the rest of the protein through the pore. Examples of T5SS adhesins include invasin from *Yersinia ruckeri* and the AIDA-I from *Escherichia coli* [3]. The second – and more recently appreciated – method of nonfimbrial secretion is the T1SS, which is used by the exceptionally large, calcium-dependent adhesins of the RTX family (Figure 1) [4–10].

RTX Proteins and Their Type 1 Secretion Signal

RTX adhesins are a subgroup of the RTX protein family that is mostly comprised of cytolysins and cytotoxins produced by many Gram-negative species as diffusible agents in the internecine struggle for survival that bacteria experience [11,12]. These RTX toxins characteristically contain an N terminal catalytic domain, typically a lipase or protease, followed by blocks of RTX repeats. While the RTX adhesins have a different domain architecture that lacks the lysin and toxin modules, the RTX repeats are conserved between both the smaller proteins and the

[1]Laboratory of Self-Organizing Soft Matter, Laboratory of Macromolecular and Organic Chemistry, Laboratory of Physical Chemistry, Department of Chemical Engineering and Chemistry, Institute for Complex Molecular Systems
[2]Department of Biomedical and Molecular Sciences, Queen's University, Kingston, Ontario K7L 3N6, Canada

*Correspondence:
daviesp@queensu.ca (P.L. Davies).

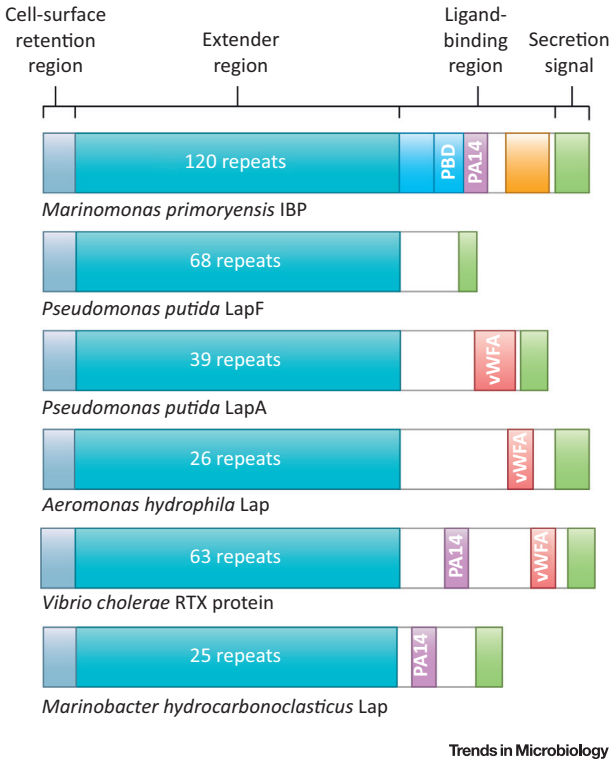

Figure 1. General Domain Architecture of RTX Adhesins. The RTX adhesins share a common domain architecture: a C terminal secretion signal and accompanying RTX repeats for transport through the type 1 secretion system (T1SS) (green); followed by the ligand-binding region, which is the most variable part among different RTX adhesins; a central extender region composed of many repeating units (cyan); and an N terminal cell-anchoring region (gray). Representative ligand-binding domains with known or predicted structures in these six RTX adhesin examples are the sugar-binding PA14 domain (magenta), the von Willebrand Factor (vWFA) domain (pink), and, within *Mp*IBP, the peptide-binding domain (PBD) (blue), and the ice-binding domain (orange). Parts of the ligand-binding region in white may contain domains of unknown structure and functionality. Abbreviation: IBP, ice-binding protein.

adhesins, giving the family its name. Conventional RTX repeats are tandemly repeated glycine- and aspartate-rich nonapeptides with a consensus sequence of GGxGxDxUx, where x indicates any amino acid and U is typically a large hydrophobic residue. Each pair of RTX repeats forms an 18-residue coil of β-roll structure with Ca^{2+} coordinated on the inside down both sides of the solenoid (Figure 2A,B).

At the C terminus of the RTX protein is a 50- to 100-residue noncleavable T1SS signal sequence. It has been suggested that the T1SS signal sequences might have more than one function. They can initiate the secretion of substrates by interacting with the T1SS translocase complex, comprised of an inner-membrane ABC transporter and the periplasmic membrane-fusion protein (MFP). This interaction can subsequently trigger the recruitment of the outer membrane protein (OMP) to form a contiguous tunnel that spans the bacterial envelope [13,14]. The T1SS signal sequence is the first part of the protein to be exported to the extracellular milieu during the translocation process [15], where it can act as the folding nucleus for the rest of the protein by folding in a Ca^{2+}-dependent manner. This would be a second function for the signal sequence. Indeed, deletion of the T1SS signal sequence not only stalls the secretion, but can severely affect the successive folding of other domains of the protein [16].

RTX toxins and RTX adhesins are similar in this export region. For example, following the classic RTX β-roll of the RTX toxin produced by *Bordetella pertussis* (CyaA) is the T1SS signal sequence localized to the C terminal ~75 residues of the toxin [17]. This module is comprised of two pairs of antiparallel β-strands and two α-helical elements (Figure 2A,D) that are required for the correct folding and biological activity of CyaA [16]. The T1SS signal module of the toxin also serves as the capping structure for the RTX β-roll [18], which helps to stabilize the solenoid

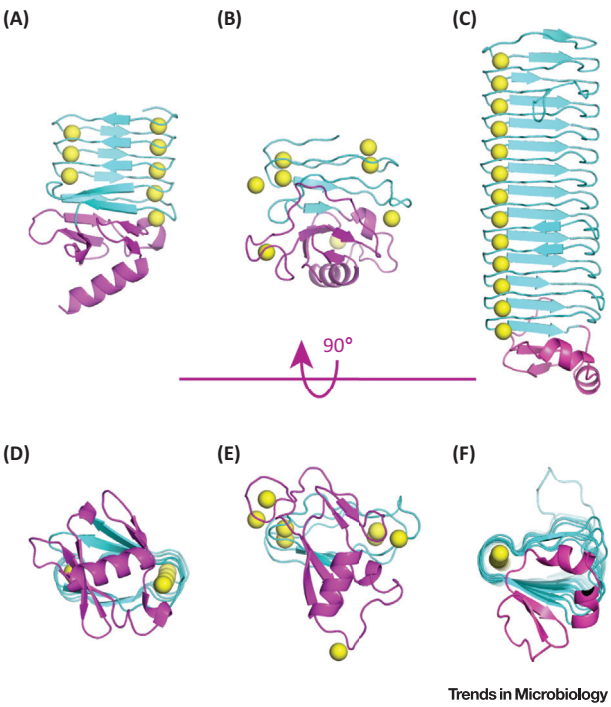

Figure 2. Type 1 Secretion System (T1SS) Domain Comparisons. Structure of the C terminal domains of CyaA and *Mp*IBP. (A) Structure of the C terminal domain of CyaA of *Bordetella pertussis* (PDB: 5CVW). The N terminal RTX β-roll is colored cyan, whereas the C terminal T1SS signal sequence is colored magenta. Calcium ions are represented by gold spheres. (B) Structure of C terminal RTX repeats and T1SS sequence of *Mp*IBP (PDB: 5JUH). The same color scheme is used as in (A). (C) Structure of the ice-binding domain of *Mp*IBP. (D,E,F) The structures are rotated 90° around a horizontal axis to show the face of the capping motifs in (A), (B), and (C), respectively.

by preventing it from forming amyloid-like aggregates [19]. Despite the absence of sequence homology, the T1SS signal sequence of the RTX adhesin, produced by *Marinomonas primoryensis* [20], referred to here as an ice-binding protein (*Mp*IBP), also contains a capping moiety with similar antiparallel β-strands and α-helices (Figure 2B,E) that is thought to serve the same functions.

Although the RTX β-roll is not required for the substrate translocation by T1SS, it plays a crucial role in enhancing secretion efficiency [21,22]. Given its high content of acidic residues, the RTX module is overall negatively charged in the absence of Ca^{2+}. This might facilitate the extrusion of RTX proteins from the outer opening of T1SS by electrostatic repulsion from the negatively charged lipopolysaccharide [16]. Once the RTX domain enters the extracellular milieu, it folds, upon binding Ca^{2+}, to form a stable β-roll, which creates steric hindrance to prevent it from sliding back into the cell by Brownian motion.

Variable Ligand-Binding Region Determines the Biofilm Niche and Its Cohabitants

The ligand-binding region near the C terminal end of the RTX adhesin is the most varied part. Here the type and arrangement of the domains seem to have been shuffled over evolutionary time, making the adhesins distinct from one another. This is true of the six examples illustrated in Figure 1. In many cases, the presence and identities of ligand-binding domains and/or their ligands have yet to be determined. As the adoption or incorporation of DNA for different

domains can change the targeting of a bacterium, the ligand-binding region is presumably under strong selective pressure. In this way, the general RTX adhesin architecture (the other three regions) can be seen as a common scaffold to house and properly present varying ligand-binding modules, which can be swapped in and out as bacterial populations/species evolve to meet new environmental needs. Presented below are a few of the domains that recur frequently within the ligand-binding regions of RTX adhesins, possibly indicating a shared functionality amongst their bacterial hosts.

PA14 Sugar-Binding Domain

Many RTX adhesins contain the PA14 sugar-binding domain, which might target cells to extracellular polysaccharides in biofilms, to carbohydrate substrates, or to surface glycolipids or glycoproteins on various cell types (Figure 1). Originally discovered as a domain of unknown function in the protective antigen (PA) toxin from *Bacillus anthracis*, the domain has been found in proteins from many different organisms, ranging from bacteria and yeast, to more complex eukaryotes like humans [23,24]. The involvement of PA14 in microorganism adhesion has been well documented in the yeasts *Saccharomyces cerevisiae* and *Candida glabrata*, where its sugar-binding function is used for self-adherence (flocculation) and human cell adhesion, respectively [25–27]. In fact, it is in yeast that the majority of PA14 structural information has been attained, namely in the flocculin proteins Flo1 and Flo5 (PDB: 4GQ7 and 2XJP) [27,28] and the epithelial adhesins EpA1, EpA6, and EpA9 (PDB: 4ASL, 4COY, and 4CP0) [26,29]. Analysis of these yeast PA14 structures has revealed a highly-conserved double aspartic acid motif which anchors a critical calcium ion that coordinates carbohydrates via two vicinal, equatorially-oriented hydroxyl groups. This same motif is present in all known RTX adhesin PA14 domains, including those from *Marinobacter hydrocarbonoclasticus*, certain *Vibrio cholerae* strains, and *M. primoryensis*, the last of which is currently the only structurally characterized PA14 within an RTX adhesin [20]. The structure of this domain (PDB: 5J6Y) is shown in magenta in Figure 3 with a close-up view of where glucose is bound.

von Willebrand Factor A Domains

Another commonly occurring domain in RTX adhesins (Figure 1) is the von Willebrand Factor A-like (vWFA) domain, a known peptide-binding fold found in many eukaryotic proteins. Several characterized RTX adhesins contain this domain – such as LapA from *Pseudomonas fluorescens*, and the RtxA protein from *Legionella pneumophila* [30,31]. Although the role of the vWFA in RTX adhesins has yet to be identified, well characterized vWFA proteins from eukaryotes, such as the titular von Willebrand Factor in blood [32] and the integrin family of cell-to-cell adhesion proteins [33], provide suggestions. In both of these eukaryotic multi-domain proteins, the vWFA module encompasses a small portion of the total sequence, forming a Rossman fold (an antiparallel β-sheet surrounded by α-helices) that can bind to extracellular matrix (ECM) proteins such as collagen [34–37]. The vWFA domain in bacteria might be used to bind to similar proteins, which would be especially useful for bacterial pathogens that infect animals. Examples of bacterial vWFA domains capable of binding human ECM proteins have been observed [38], as has the conservation of the serine-coordinated calcium ion, known as the metal-ion-dependent adhesion site (MIDAS), which allows integrins to bind acidic residues on their target proteins [39].

An alternative role for vWFA domains in bacteria is inspired by the von Willebrand Factor protein, and its use as a mechanosensor in blood clotting. The high shear forces associated with an open, bleeding wound leads the vWFA1 domain of the protein to become slightly unfolded, revealing a binding site for a glycoprotein on the outside of platelets [40–42]. The platelets can thereby cluster around the wound, facilitating clotting. Interestingly, a vWFA

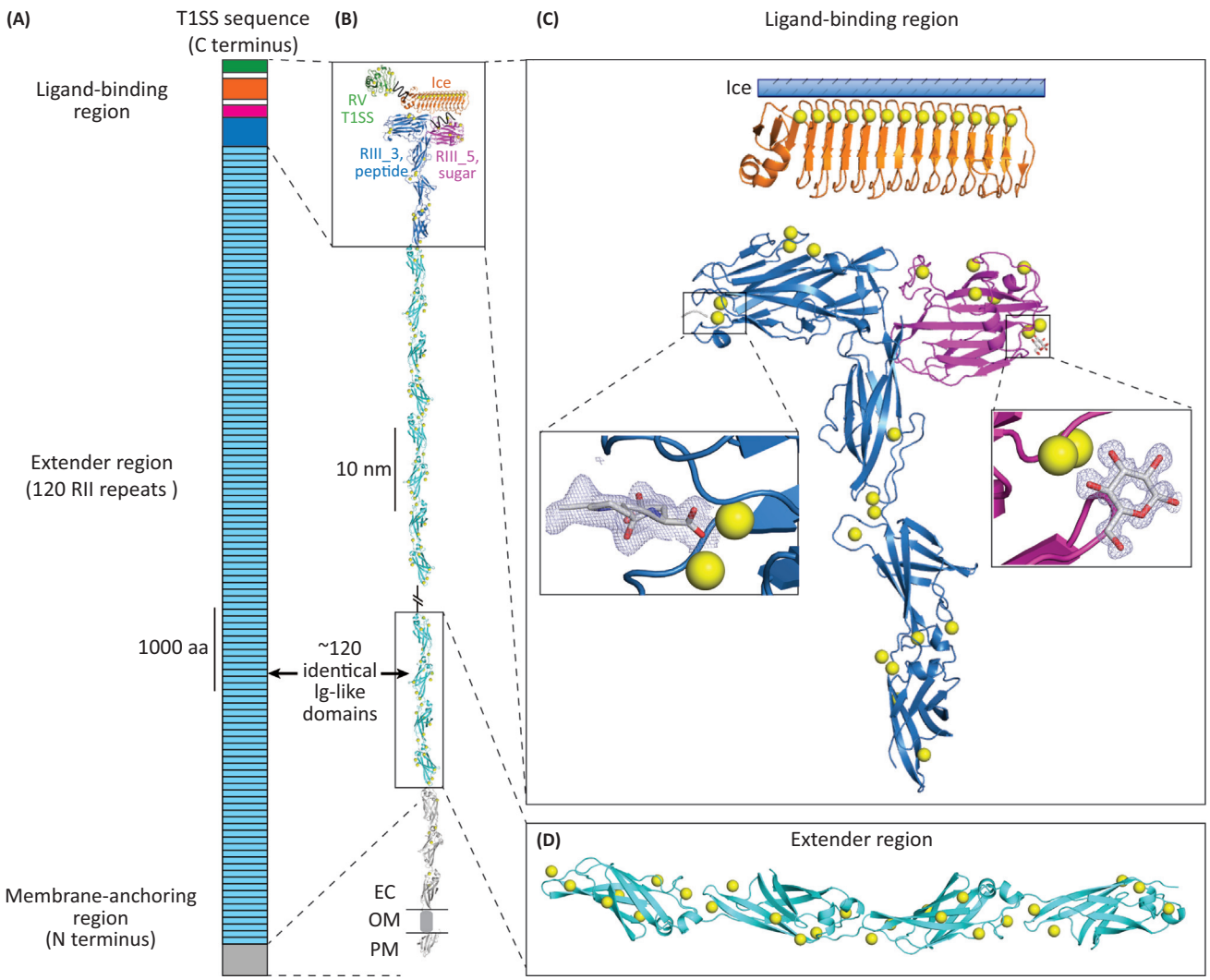

Figure 3. Road Map of the *Mp*IBP Ice-Adhesin Showing Four Functional Regions. (A) Linear domain map of *Mp*IBP drawn to scale. The membrane-anchoring region at the N terminus is colored gray. The ~120 repeats that span the central extender region are colored cyan. In the ligand-binding region, the peptide-binding region is colored dark blue, the sugar-binding domain is colored magenta, while the ice-binding domain is colored orange. The type 1 secretion system (T1SS) sequence at the C terminus is colored green. The small white regions near the C terminus are linkers with no known three-dimensional structures. (B) NMR and X-ray crystal structures of linked *Mp*IBP domains from N to C termini are shown in cartoon representation. The same color scheme is applied as in (A). Near the N terminus, the small-angle X-ray scattering (SAXS) structure of the T1SS-β-barrel-spanning module of *Mp*IBP is illustrated as a gray cylinder. Outer membrane (OM) is indicated by horizontal lines on either side of the *Mp*IBP T1SS-β-barrel-spanning module. EC and PM refer to extracellular and periplasmic locations. Hatched lines indicate the ~108 central repeats that are not shown in the figure. The linker regions near the C terminus are indicated by wavy lines. (C) Zoomed-in view of the ligand-binding region of *Mp*IBP. The same color scheme is used as in (B). Ca^{2+} ions are indicated as yellow spheres. The insets show enlarged views of the peptide (left) and sugar (right) molecules anchored to the ligand-binding domains and shown in stick representation (carbon atoms in white, oxygen atoms in red, and nitrogen atoms in blue) with $2F_o–F_c$ map countered at 1 σ (blue mesh). (D) A segment of four linked Big domains from the extender region showing Ca^{2+} ions as yellow spheres, both within and between the β-sandwich domains. Adapted from [20].

domain-containing protein – PilY – from *Pseudomonas aeruginosa* has been proposed to function similarly, but as a detector for the heightened mechanical shear forces surrounding a surface [43,44]. Pre-exposing *P. aeruginosa* to a surface increases the bacterium's subsequent virulence during amoeba infection. Siryaporn *et al*. showed that activation of this virulent

phenotype can be prevented through the deletion of the PilY protein: a surface-exposed protein required for pili biosynthesis that contains an N terminal vWFA domain [43,44]. However, deletion of the vWFA, alone, led to a hypervirulent strain that did not require pre-exposure to surfaces to increase pathogenicity. Taken together, the vWFA domain appears to act as a surface-sensing switch, keeping the virulence phenotype deactivated until a sufficient shear force is sensed in the presence of a surface.

The biophysical mechanisms at play in *Pseudomonas* are not yet explained, nor is it known how widespread this supposed vWFA-dependent strategy of surface-sensing is in bacteria. While no other examples have been presented so far, *Caulobacter crescentus* relies on the resistance 'felt' during pili retraction to sense and irreversibly adhere to a surface [45]. The protein that is predicted to anchor the pili to the peptidoglycan layer (TadG) also contains a predicted vWFA domain [46,47]. While the RTX adhesins have a very different architecture than both the PilY and TadG proteins, this interesting alternative function should be considered in future studies.

RTX-Derived Ice-binding Domain and Homologs of Unknown Function

The feature that led to the discovery of the massive RTX adhesion in the Antarctic bacterium *M. primoryensis* was the presence of a domain that avidly binds ice [48]. This seems to have evolved from the nearby C terminal β-roll, possibly after a gene duplication event (Figure 2C). While the RTX sequences in the β-roll aid secretion [16] (Figure 2B), RTX repeats in this larger more proximal domain have evolved the remarkable ability to bind ice, leading to the adhesin's designation as the *M. primoryensis* ice-binding protein (*Mp*IBP). In contrast to the conventional β-roll fold with two flanking rows of Ca^{2+}, each 19-residue coil of the ice-binding domain contains only one RTX repeat, resulting in a β-solenoid structure with 13 Ca^{2+} aligning down only one of its flanks (Figure 2C). The single RTX repeats in these coils have diverged to have a consensus of xGTGND (in contrast to the classic GGxGxD), where the Thr-Gly-Asn/Asp motif helps to form a flat surface that runs the length of the β-solenoid [48]. The X-ray crystal structure of this ice-binding domain revealed that the array of outward-pointing Thr organizes cages of water molecules around the methyl groups that are then hydrogen-bonded to nearby hydrophilic groups into an ice-like pattern that merges with, and freezes to, the quasi-liquid layer of water coating the ice lattice [49]. These 'anchored clathrate waters' are able to freeze *Mp*IBP to several planes of ice.

Homologs of this β-solenoid ice-binding domain are present in the RTX adhesin of at least one other *Marinomonas* species, *M. ushuaiensis*, but without the regularly spaced Thr and Asn arrays that are essential for ice-binding. The same domain has popped up further afield in a magnetotactic bacterium RTX adhesin, but again without the ice-binding residues (GenBank: BAE50805). Other RTX domains with ligand-binding potential have also been identified. CyaA produced by *B. pertussis* has five distinct blocks of RTX repeats separated by linkers ranging between 23 and 49 residues in length. Two of the central blocks have evolved to be integrin-binding domains [50], while the C terminal block facilitates the proper secretion and folding of the whole protein [51]. Intriguingly, using ribosome display, Bulutoglu *et al*. showed that the C terminal block can be turned into a lysozyme-binding module with an apparent dissociation constant of 65 nM [52]. This *in vitro* evolution study further demonstrated the high degree of plasticity of these β-rolls to evolve adhesion capabilities for various ligands found on cells or other surfaces.

Uncharted Adhesion Domains

Bioinformatic analyses of C terminal regions for both studied and hypothetical adhesins reveal large stretches of sequence that do not belong to a known domain family (Figure 1).

Interestingly, PSI-BLAST searches of these regions to probe for distantly related sequences often show definitive breaks in homology, implying the amalgamation of multiple sequences from different sources. Indeed, such breaks fit with the concept of a modular ligand-binding region prone to switching domains as needed. To date, only a few identifiable domains have been structurally and functionally characterized (above). The mystery regions between known domains may be hiding previously unknown structures and binding partners and will require study if the role of individual RTX adhesins in the life cycle of their hosts is to be understood.

As an example, a different type of peptide-binding domain was discovered serendipitously when solving the structure of the *M. primoryensis* adhesin (Figure 1). This calcium-dependent β-sandwich domain (PDB:5K8G), of previously unknown structure and function in the ligand-binding region of the adhesin, was observed to have a binding pocket in which the C terminal peptide of a second molecule in the crystal was bound (Figure 3) [20]. The discovery and characterization of this domain – as can be said for the resolution of any mystery region – is applicable beyond one adhesin, as a domain homolog can be found in the RTX adhesins of several *Vibrio* species.

The Ultrastructure of an RTX Adhesin Ligand-Binding Region

*Mp*IBP is the first RTX adhesin in which the entirety of the ligand-binding region has been both structurally and functionally characterized [20]. In *M. primoryensis*, this ligand-binding region serves at least two functions. It binds the bacteria to ice but also to the Antarctic diatom, *Chaetoceros neogracile* [53] (Figure 4). The latter function requires adhesin attachment to terminal sugars and peptide moieties on the surface of the diatom. Thus the sugar, peptide, and ice-binding domains near the C terminal end of the adhesin facilitate the formation of a mixed species microcolony on the underside of sea or lake ice to the benefit of both contributing species. The diatoms occupy an optimal niche for photosynthesis thanks to the bacteria's ability to bind them and ice at the same time, and are treated to essential nutrients, such as vitamin B12, secreted by the bacteria [54,55]. Likewise, the aerobic bacteria potentially benefit from the oxygen and other waste products of the diatoms.

Six distinct domains are present in this region of *Mp*IBP, three of which are ligand-binding (Figure 3C). At the proximal end of this grouping are five β-sandwich-like domains (RIII_1 to RIII_5). They are not an extended 'beads-on-a-string' structure, but are instead organized into a T-shape, where structural domains RIII_1 and _2 make up the stalk of the T, while RIII_4 sits at the junction to project the two ligand-binding domains (RIII_3 and _5) away from each other (Figure 3). RIII_3 and _5 form the tips of the T-shape, with RIII_3 being the peptide-binding domain, and RIII_5 the PA14 sugar-binding domain, both described earlier. The two adhesion domains require Ca^{2+} to coordinate their respective ligands, a common theme amongst RTX adhesin domains. The stringent way in which these domains are organized in 3D space suggests that the T-shape is designed to extend the ligand-binding domains away from each other to allow contact with one substrate or the other, but not both side by side (Figure 4). This organization is similar at one level to that of the IgG antibody where two antigen-binding sites are projected away from each other. It is likely that multidomain ultrastructures like this will be found in other adhesin ligand-binding regions. It may be necessary to crystalize the entire region as a unit, or, if that is not possible, to amalgamate individual domains into the whole using small-angle X-ray scattering (SAXS) envelopes.

The sixth domain of *Mp*IBP, the ice-binding, calcium-coordinated β-solenoid, is closely linked by ~80 residues to the other five domains. It is not clear at this point if the ice-binding domain is part of a higher structure with the other five domains or is just connected to them by a linker.

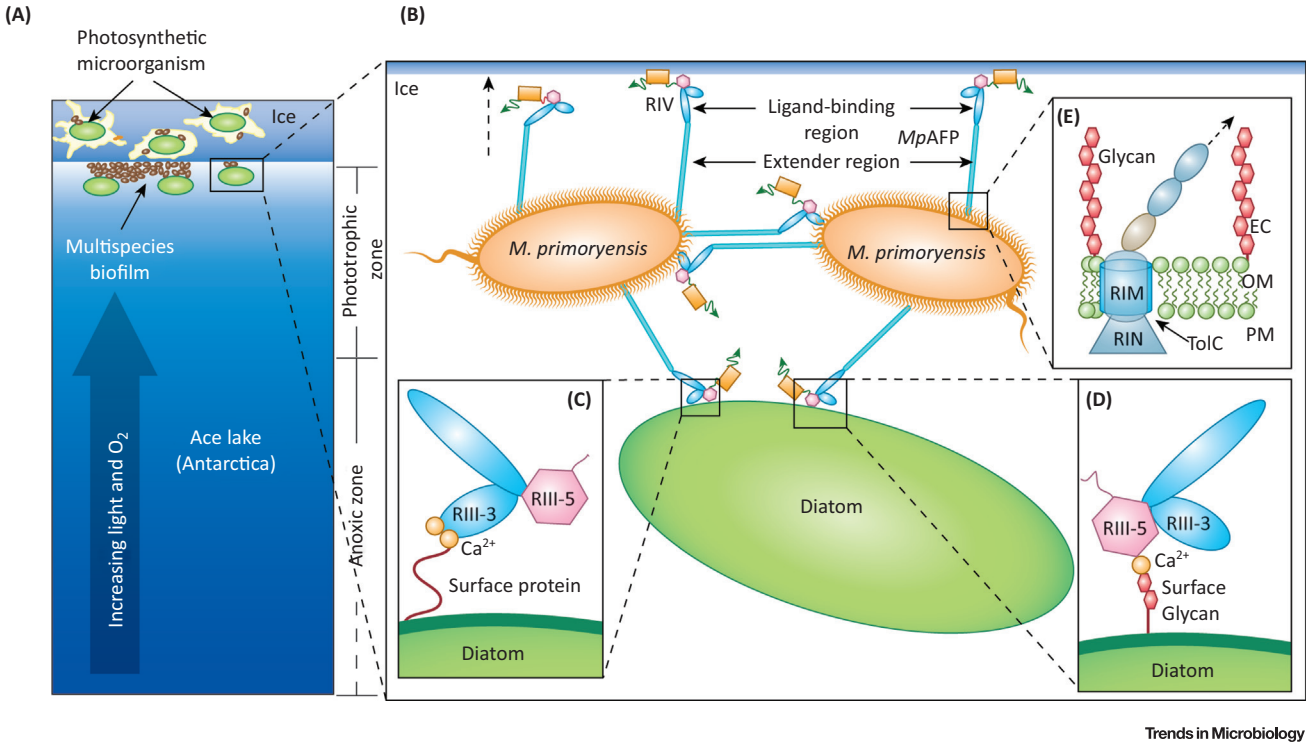

Figure 4. Schematic of *Mp*IBP Binding *Marinomonas primoryensis* and Diatoms to Ice. (A) Ice/snow that covers the water surface in Antarctica (e.g., Ace Lake) is represented by a gray rectangle with three internal brine channels of irregular shape. Lake water is colored blue with a light to dark gradient from top to bottom signifying the increased availability of light and oxygen towards the top of the water column as indicated by the gray arrow. Bacteria and photosynthetic microorganisms such as diatoms within the brine pits and underneath the ice are drawn as small white ovals and large green ovals, respectively. The phototrophic and anoxic zones are indicated on the right. (B) Expanded view of (A) showing two linked bacterial cells bound to ice and a diatom. Cell-surface proteins and carbohydrates are drawn as fuzzy black hairs, and the polar flagella are drawn as squiggles. *Mp*IBPs protrude from cell surfaces. The extender region, peptide-binding region, sugar-binding domain, ice-binding domain, and type 1 secretion system (T1SS) sequence are drawn as cyan rods, blue ovals, magenta hexagons, orange rectangles, and dark green triangles, respectively. (C) Enlarged view of *Mp*IBP peptide-binding domain (PBD) interacting with a protein on the cell surface of a diatom. Ligand-binding Ca^{2+} ions are drawn as yellow spheres. Surface protein is indicated by a wavy line from the cell surface. (D) Enlarged view of *Mp*IBP sugar-binding domain (SBD) interacting with a sugar molecule on the cell surface of a diatom. Ligand-binding Ca^{2+} ions are drawn as yellow spheres. (E) Expanded view of the membrane-anchoring domains of *Mp*IBP (gray triangle, cylinder, and ovals) near the outer membrane (OM). RIN is the N terminal domain of the retention region that cannot pass through TolC. RIM is the middle domain of this region that becomes lodged within the tunnel of TolC. Surface glycans are drawn as connected brown hexagons. The hollow T1SS β-barrel pore through the OM is outlined in black. Arrow with a broken line indicates that the protein continues to the C terminus of *Mp*IBP. Adapted from [20].

However, the sixth domain is too close to the T-shaped structure to permit simultaneous binding of one adhesin to both ice and a diatom. For this dual binding to occur, *M. primoryensis* must have at the very least two RTX adhesins expressed, as shown in Figure 4, with one directed to the ice and another to the diatom.

Extension Region: Tandem Big Domains Extend the Reach of the Adhesin

A striking feature of the RTX adhesin domain architecture is the central region, which often accounts for the majority of the proteins' molecular weight. This segment houses varying numbers of tandem repeats that most often fold as a 10–15 kDa β-sandwich, similar to those found in immunoglobulins, which explains their general title of bacterial immunoglobulin-like (Big) domains. Big domains are prevalent in many species of Gram-negative bacteria, and are used in RTX adhesins to extend the substrate-binding C terminal domains into the extracellular space, away from the cluttered cell membrane of the bacterium.

Calcium Rigidifies and Strengthens the Extender Region

To maintain effective extension from the cell surface, it stands to reason that extender regions require a relatively rigid, elongated conformation [56]. Several structures of extender region fragments from RTX adhesins have been solved to date, including a construct containing three tandem BIg repeats from the SiiE adhesin of *Salmonella enterica* [57], and another containing four tandem BIg repeats from *Mp*IBP, denoted as the *Mp*IBP tetra-tandemer [58]. Both structures revealed the expected β-sandwich domains to be aligned in extended rods, with calcium ions coordinated in the flexible linkers between domains (Figure 3D). These ions were hypothesized to rigidify the tandem repeats, thereby facilitating an extended structure that prevents the adhesin from bending back on itself and interacting with its own cell surface. Indeed, molecular dynamic simulations and electron microscopy of the full-length SiiE showed an extended rod-like structure in solution, which was compromised by a loss of calcium [57]. Similarly, biophysical analysis of the *Mp*IBP tetra-tandemer using size-exclusion chromatography, analytical ultracentrifugation (AUC), and SAXS all demonstrated an apparent increase in rigidity upon calcium binding [58].

Aside from rigidifying the flexible linkers, calcium can also contribute to the strength of the BIg domain fold. Most domains in RTX adhesins require calcium to fold properly. Massive changes in secondary structure, from random coil to predominantly β-strand, can be seen during the titration of *Mp*IBP BIg domains with calcium monitored by circular dichroism spectroscopy [56,58]. The resulting β-sandwich domains of Ca^{2+}-bound *Mp*IBP can withstand forces as high as 350 pN without unfolding, as seen through single-molecule force spectroscopy experiments of an octa-tandemer of *Mp*IBP under high calcium conditions [59]. Such a resistance to unfolding is remarkable, outclassing the folding strength of even the Ig-like domain I27 of the human muscle protein titin by ~120 pN [60,61]. BIg domains from other RTX adhesins seem to share this folding strength, such as *Mh*Lap from the oil-degrading bacterium *M. hydrocarbonoclasticus* [59]. The structural element proposed to allow these β-sandwich domains to attain such high stability in the face of intense shear forces is an altered form of the classic mechanical clamp: hydrogen-bonded parallel β-strands found at the termini of the domain [62,63]. This motif is found in many stably folded β-sandwich domains, including I27 from titin, and the extender domains of *Mp*IBP. The latter structure also shows coordinated calcium ions flanking the clamps that make additional contacts. Further single-molecule force spectroscopy experiments showed that the *Mp*IBP octa-tandemer in low-calcium conditions unfolds under forces roughly similar to titin I27, supporting the added value of the calcium-mediated shear clamp motif. Additionally, the BIg domains of SiiE, which appear to lack the C terminal calcium-mediated shear clamp, unfold at a much lower value of ~120 pN [57].

Variability amongst Adhesin BIg Domains

Though the presence and proposed biological role of the extender region appears universal to all RTX adhesins, the number of repeats present can vary fivefold (Figure 1). It is not clear why certain adhesins contain tens of repeats (e.g., *Mh*Lap has ~25 repeats), while others have over a hundred (e.g., *Mp*IBP is estimated to contain ~120). Several hypotheses can be put forward to explain the varied lengths of the extension region in RTX adhesins. (i) Different bacteria–substrate interactions may require different degrees of proximity. For instance, the smaller non-RTX adhesion protein intimin maintains few repeat domains to facilitate close contact between cells, which may not be necessary (or advantageous) for adhesion to other substrates [64]. (ii) Different bacteria express macromolecules on their surfaces of varying lengths [e.g., lipopolysaccharide (LPS), other adhesins, fimbriae etc.], thereby changing the extension required for an adhesin to out-reach potentially interfering surface components. (iii) Certain BIg domains may

have additional functions beyond extension. The SiiE adhesin BIg domains are capable of adhering to sugar-containing ligands in a lectin-like manner, as shown via lectin blockade experiments [65]. This gives an additional adhesion role to the region, and may partially explain the requirement of many SiiE repeats for effective invasion. Which (if any) of these hypotheses answers the question of repeat number will require further study.

It is also possible that the vast difference in repeat number is indicative of a lack of evolutionary selection, implying that the exact number of repeats is unimportant to adhesin function and therefore left to the whims of DNA duplication and recombination. That said, it seems unlikely that organisms such as *M. primoryensis,* which produce upwards of a hundred repeats, would invest energy in producing a 1.5 MDa protein if it were not beneficial. Indeed, it has been observed that the ability of SiiE – which contains 56 repeats – to facilitate invasion of *S. enterica* into epithelial cells declines if even five repeats are removed [66].

The sequence identity shared between repeats within the same adhesin is almost as variable as the number of repeats, ranging from low values of 40–60% at the amino-acid level (e.g., LapF), to 100%, even at the *nucleotide* level (e.g., *Mp*IBP, *V. cholerae* str. FORC_055 adhesin GENBANK: WP_096070493). For the adhesins with many nearly-identical repeats, the inability of most DNA sequencing methods to acquire sequencing reads long enough to cover the whole extender region can stymy attempts at assembling the reads into one contiguous sequence. Wrobel *et al*. found that the number of Ig-like repeats present in the invasin-like autotransporter adhesin from *Y. ruckeri* was underestimated by the short sequencing reads of Illumina sequencing, requiring the exceptionally long reads of Pacific Bioscience sequencing to attain a correct number [67]. *Mp*IBP serves as a notable case study for this problem, as the total number of identical 312 bp repeats in its long extender region could not to be determined, even by PacBio sequencing [20,68]. Interestingly, while the older sequencing methods were simply unable to connect the two ends of *Mp*IBP, the genome analysis software used to assemble the PacBio sequencing data of *M. primoryensis* provided a supposed 'complete' *Mp*IBP, with the N and C termini connected by 75 BIg repeats. However, upon closer examination, this assembly simply used the maximum number of repeats through which the sequencing was able to read, and is therefore not representative of the actual number of BIg domains in *Mp*IBP. This false assembly would be hard to detect if one were not looking for it, potentially calling into question other such 'completed' adhesin sequences. It is unclear how often difficult cases like the *Mp*IBP gene sequence occur; but we have noted examples of sequencing maladies caused by highly identical sequences in other adhesin genes. The N and C termini of *Mp*IBP homologs from *Marinomonas* species *M. profundimaris* and *M. blandensis* str. MED121 are split into two contigs, leaving gaps in the genomic sequence [69,70]. Similarly, an RTX adhesin in *Magnetospirillum magneticum* has a sequencing gap in its extender region sequence [71].

The inability to trust the assembled sequence of some adhesin genes may require in-depth scrutiny of an individual extender region. To estimate the number of repeats in the extender region of *Mp*IBP, the gene was restriction-digested using four-cutter enzymes that cut immediately outside the extender region, but not within. This digest yielded the full-length extender region to be resolved and measured by pulsed-field gel electrophoresis. By frequently changing the direction of the current during electrophoresis, this method enables large DNA fragments to pass through the gel and be accurately sized alongside large DNA standards like the genome of lambda phage. Using pulsed-field gel electrophoresis, *Mp*IBP was found to contain ~120 repeats [68].

Cell-Surface Retention Region: A Calcium-Independent Plug Anchors the Adhesin in the T1SS OMP

Cell fractionation analyses suggested that the RTX adhesin LapA produced by *P. fluorescens* is retained on the outer membrane [72,73]. However, the mechanism of how these adhesion structures are localized to the cell surface remained a mystery until recently. Given that RTX adhesins require T1SS for translocation to the cell surface, Guo *et al*. reasoned that these giant proteins might be anchored there by interacting with a component of the secretion machinery [20].

This hypothesis has been supported by structural studies on *Mp*IBP. T1SS secretes its substrates with a C-to-N-terminal directionality [15], thus it is likely that the domains responsible for cell-surface retention are near the protein's N terminus after most of the adhesin has been extruded into the medium (Figure 4). Using a combination of NMR and SAXS, Guo *et al*. showed that the N terminal domain of *Mp*IBP folds as a stable β-sandwich with a triangular cross-section (30 Å × 29 Å); whereas the adjoining domain on the C terminal side has a slim cylindrical neck shape with a diameter of roughly 18 Å [20]. This cylinder can snugly fit into the TolC, the outer-membrane β-barrel of the T1SS apparatus with an internal diameter of ~20 Å [74,75]. But the β-sandwich plug cannot pass through the TolC pore because of steric hindrance, thereby blocking the total release of the giant adhesin to the medium (Figure 5). In contrast to all the other >120 domains of *Mp*IBP that are unstructured during secretion and require Ca^{2+} for folding, the N terminal plug and neck domains are folded in the absence of Ca^{2+} before entering the T1SS tunnel. This finding provided the structural basis for what seems to be a general mechanism widely used by Gram-negative bacteria to retain large adhesins on their cell surface [76]. In this paradigm, the many distal parts of the adhesins protrude from the cell surface to interact with the environment, while the N terminal plug domain is anchored on the periplasmic side of the outer membrane via the T1SS-β-barrel-spanning module.

This structural model has been experimentally validated by Smith *et al*. who performed *in vivo* secretion competition experiments between the 0.8-MDa RTX adhesin LapA produced by *P. fluorescens* and the C terminal secretion domain of LapA tagged with a three-hemagglutinin epitope (HA-C235) [76,77]. The rationale for this experiment was that if the surface-retention of LapA is achieved by plugging the T1SS duct, the secretion of HA-C235 may be affected as the two substrates share the same secretion machinery. Indeed, when the native LapA was held to the cell surface, the secretion level of HA-C235 was greatly reduced. However, HA-C235 secretion was resumed when the N terminal plug domain of LapA was cleaved off by a periplasmic protease (LapG). This is because proteolysis released LapA to the medium and freed up the T1SS channels for the export of HA-C235. Moreover, it was demonstrated that the secretion of HA-C235 can be restored when the T1SS machinery proteins are overexpressed in *P. fluorescens*, further consolidating the proposed model that the N terminal domain retains RTX adhesins by plugging and occupying the T1SS channel.

Detailed structural analysis of the plug domain of *Mp*IBP revealed that it contains several outward-pointing phenylalanine residues, which might directly interact with the outer membrane to help anchor the adhesin. With relatively low sequence identities (~20%), the 3D fold of the plug domain is conserved in the RTX adhesin from many bacteria, including pathogens such as *V. cholerae*, *P. aeruginosa,* and *Shewanella oneidensis* [20,76]. In fact, plug domains from the *V. cholerae* or *P. aeruginosa* adhesins are capable of anchoring chimeric LapAs to the cell surface of *P. fluorescens*. In contrast to the stable β-sandwich plug, its neighboring cylindrical β-barrel-spanning module is flexible and labile to proteolysis [20,76]. Indeed, a specific proteolytic site between the 2nd and 3rd positions of the conserved sequence of Thr

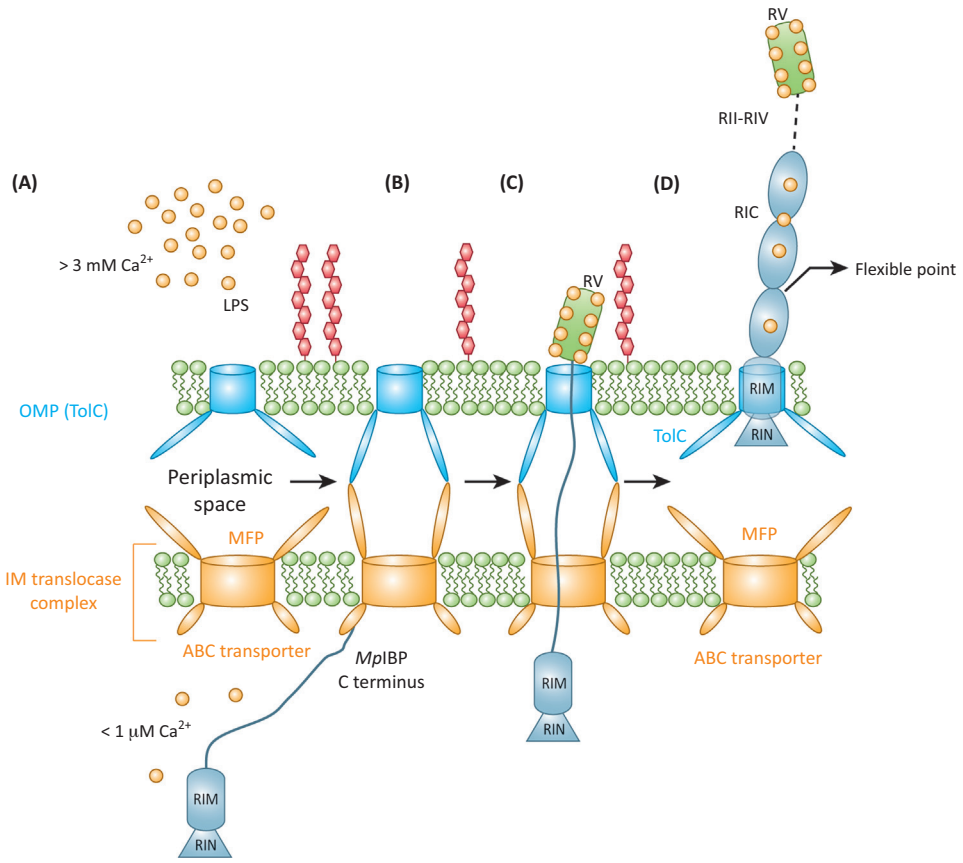

Figure 5. Retention of RTX Adhesin in the Bacterial Outer Membrane. (A) In the type 1 secretion system (T1SS), a membrane fusion protein (MFP) and an ABC transporter form a stable translocase complex anchored to the inner membrane (IM). (B) Upon contact with the unstructured C terminal sequence of *Mp*IBP or another T1SS substrate, this translocase complex undergoes conformational changes to recruit the T1SS outer membrane protein (OMP), TolC, and forms a continuous channel across the cell envelope. (C) Most of the *Mp*IBP sequence remains unstructured in the secretion channel, but folds upon entering the Ca^{2+}-rich extracellular environment. In contrast, the N terminal plug (gray triangle) and β-barrel-spanning (gray cylinder) domains are structured in the absence of Ca^{2+} during secretion. (D) When the entire T1SS substrate has passed the IM–translocase complex, the T1SS machinery can disassemble, leaving the β-barrel-spanning module inserted in the TolC pore, while the N terminal plug module prevents the total release of *Mp*IBP by steric hindrance. Adapted from [89]. LPS, lipopolysaccharide.

(Pro)-Ala-Ala-Gly can be activated to release the bacterium from its biofilm when growth conditions are unfavorable, which allows it to become planktonic in the search for a better niche [72,78]. Although the above model represents a widely used mechanism for surface retention, it should be noted that some RTX adhesins have evolved modified surface-release strategies. For example, the giant adhesin SiiE from the human pathogen *S. enterica* uses a predicted coiled-coil moiety in place of the β-sandwich plug to transiently hold the protein to its T1SS apparatus [65,79]. With no predicted proteolytic site, it remains unknown what triggers the release of SiiE into the medium. Intriguingly, although a T-A-A-G site for proteolysis is present in the non-RTX adhesin of P. aeruginosa (CdrA), this protein is retained by a 'cysteine hook' that restricts its secretion through the outer-membrane pore via the Type Vb secretion system [80,81].

Strategies to Block Adhesion/Infection

Adhesion is a critical step in biofilm formation, which for pathogenic bacteria can lead to infection. Adhesion allows targeting of a given bacterium to a specific surface, and – in flow environments – it enables bacteria to resist physical removal by shear forces. The target specificity of the ligand-binding domains within an RTX adhesion is instrumental in guiding the bacterium to its optimal environmental niche. Blocking the ligand-binding domains of RTX adhesins is an attractive strategy to prevent surface adhesion and subsequent biofilm formation. Previously, multiple strategies have been proposed to inhibit adhesion by spoiling ligand-binding domain interactions; these include: antibodies, substrate analogs, metal-ion interference, and surface modification [82–85].

By incubating *M. primoryensis* with antibodies raised to the ice-binding domain of *Mp*IBP, which makes up only ~2% of the whole adhesin, Bar Dolev *et al*. were able to completely prevent bacteria from adhering to ice [86]. In principle, antibodies to the key surface-binding domains of other RTX adhesins could similarly prevent colonization by their bacterial hosts. The adhesins must be studied for the structure–function relationships to determine their key domains that could be used as vaccines in the prevention of infection.

Using *Mp*IBP as an exemplar, there are additional ligand-binding domains nearby in the hypervariable ligand-binding region of this RTX adhesin that contribute to biofilm cohesion. In the case of *Mp*IBP these are sugar- and peptide-binding domains that link the bacteria to diatoms to form a mixed-species biofilm (Figure 4) [20]. It is hypothesized that the two domains bind to as yet unidentified polysaccharides and proteins on the diatom surface. Therefore, it may be possible to prevent adhesion or cohesion by blocking the ligand-binding domain from associating with its appropriate substrate through competition with an analog. A precedent for this approach has been the use of nonmetabolizable mannose mimics to prevent the ligand-binding domain of a fimbrial adhesion (FimH) of uropathic *E. coli* (UPEC) from binding urothelial cells, leading to a drastic reduction in urinary-tract infections [87,88].

Concluding Remarks

The first RTX adhesin to be completely characterized at the structural level has revealed a giant protein whose evolutionary purpose is to help its host bacterium to colonize a specific niche and form a biofilm. It does this by extending a set of ligand-binding domains on a single thread-like protein hundreds of nanometers away from its anchoring point in the outer membrane. The nature of the ligand-binding domains determines the surface to which the bacteria bind and the company they keep. In the RTX adhesin of *M. primoryensis,* one domain binds to ice and two others to molecules (sugar and peptide) on the surface of a diatom. The close proximity of the three ligand-binding domains near the C terminus of the adhesin makes it unlikely that both extensive surfaces can be bound by the same adhesin, which argues that there is more than one copy of this large protein projecting from each bacterium. Bioinformatics analyses of RTX adhesin homologs in many Gram-negative bacteria show the same structure–function relationships. The adhesins emerge unfolded through the T1SS but are trapped in the outer membrane by a pre-folded N terminal domain. Most of the adhesin serves to project the ligand-binding domains into the medium in search of substrates for bacterial attachment. This region of the RTX adhesins is the most varied in structure and least recognized in terms of their binding partners. To understand infection, colonization, and biofilm formation by specific bacteria it will be essential to characterize these ligand-binding domains (see Outstanding Questions). Here there are great opportunities for interfering with infection and biofilm formation through the use of ligand competitors and antisera.

Outstanding Questions

What are the unidentified sequences in the ligand-binding regions of RTX-adhesins? They are likely to be a mixture of novel ligand-binding domains and adjunct domains that present the former in a particular orientation for binding substrates.

But what are their substrates and how can these be identified? To ask the question more broadly, have these regions been selected through coevolution with a host to have the right ligand-binding domains for life in a particular niche? The investigation of the RTX adhesin of *M. primoryensis* would suggest so, where two of the three ligand-binding domains attach the bacteria to a specific diatom and the third attaches the aggregated microorganisms to ice to form a photobiofilm. If so, we might not be able to interpret RTX adhesins in isolation but only in the context of their bacteria–host partnerships. These could be ideally studied under the microscope in microfluidic systems.

Is the binding of an RTX adhesin to its substrate(s) the first step in biofilm formation? The long reach of the adhesin with ligand-binding domains at the distal end is suggestive of bacteria putting out feelers for their substrates. Again, microfluidic systems will provide an ideal opportunity to observe the initial stages of biofilm formation once the correct participants are put together with their substrates.

Acknowledgments

This work was funded by a Natural Sciences and Engineering Research Council of Canada discovery grant to P.L.D. (RGPIN 2016-04810), and by the European Union through an ERC grant (ERC-2014-StG Contract No. 635928) to I. Voets. P. Davies holds the Canada Research Chair in Protein Engineering, and T.D.R.V. is funded by a Canadian Graduate Scholarship from the National Science and Engineering Research Council (NSERC).

References

1. Green, E.R. and Mecsas, J. (2016) Bacterial secretion systems – an overview. *Microbiol. Spectr.* Published online February 26, 2016. http://dx.doi.org/10.1128/microbiolspec.VMBF-0012-2015
2. Gerlach, R.G. and Hensel, M. (2007) Protein secretion systems and adhesins: The molecular armory of Gram-negative pathogens. *Int. J. Med. Microbiol.* 297, 401–415
3. Leo, J.C. *et al.* (2012) Type V secretion: mechanism(s) of autotransport through the bacterial outer membrane. *Philos. Trans. R. Soc. B Biol. Sci.* 367, 1088–1101
4. De Gregorio, E. *et al.* (2015) Biofilm-associated proteins: news from *Acinetobacter*. *BMC Genomics* 16, 933
5. Hinsa, S.M. *et al.* (2003) Transition from reversible to irreversible attachment during biofilm formation by *Pseudomonas fluorescens* WCS365 requires an ABC transporter and a large secreted protein. *Mol. Microbiol.* 49, 905–918
6. Martínez-Gil, M. *et al.* (2012) Calcium causes multimerization of the large adhesin LapF and modulates biofilm formation by *Pseudomonas putida*. *J. Bacteriol.* 194, 6782–6789
7. Martínez-Gil, M. *et al.* (2010) LapF, the second largest *Pseudomonas putida* protein, contributes to plant root colonization and determines biofilm architecture. *Mol. Microbiol.* 77, 549–561
8. Satchell, K.J.F. (2011) Structure and function of MARTX toxins and other large repetitive RTX proteins. *Annu. Rev. Microbiol.* 65, 71–90
9. Yoshida, K. *et al.* (2017) Biofilm formation by *Paracoccus denitrificans* requires a type I secretion system-dependent adhesin BapA. *FEMS Microbiol. Lett.* Published online February 2017. http://dx.doi.org/10.1093/femsle/fnx029
10. Syed, K.A. *et al.* (2009) The *Vibrio cholerae* flagellar regulatory hierarchy controls expression of virulence factors. *J. Bacteriol.* 191, 6555–6570
11. Lally, E.T. *et al.* (1999) The interaction between RTX toxins and target cells. *Trends Microbiol.* 7, 356–361
12. Linhartová, I. *et al.* (2010) RTX proteins: a highly diverse family secreted by a common mechanism. *FEMS Microbiol. Rev.* 34, 1076–1112
13. Balakrishnan, L. *et al.* (2001) Substrate-triggered recruitment of the TolC channel-tunnel during type I export of hemolysin by *Escherichia coli*. *J. Mol. Biol.* 313, 501–510
14. Thanabalu, T. *et al.* (1998) Substrate-induced assembly of a contiguous channel for protein export from *E. coli*: reversible bridging of an inner-membrane translocase to an outer membrane exit pore. *EMBO J.* 17, 6487–6496
15. Lenders, M.H.H. *et al.* (2015) Directionality of substrate translocation of the hemolysin A Type I secretion system. *Sci. Rep.* 5, 12470
16. Bumba, L. *et al.* (2016) Calcium-driven folding of RTX domain β-rolls ratchets translocation of RTX proteins through type I secretion ducts. *Mol. Cell* 62, 47–62
17. Mitchell, A. *et al.* (2015) The InterPro protein families database: the classification resource after 15 years. *Nucleic Acids Res.* 43, D213–D221
18. Bryan, A.W. *et al.* (2011) Structure-based prediction reveals capping motifs that inhibit β-helix aggregation. *Proc. Natl. Acad. Sci. U. S. A.* 108, 11099–11104
19. Peralta, M.D.R. *et al.* (2015) Engineering amyloid fibrils from β-solenoid proteins for biomaterials applications. *ACS Nano* 9, 449–463
20. Guo, S. *et al.* (2017) Structure of a 1.5-MDa adhesin that binds its Antarctic bacterium to diatoms and ice. *Sci. Adv.* 3, e1701440
21. Holland, I.B. *et al.* (2016) Type I protein secretion-deceptively simple yet with a wide range of mechanistic variability across the family. *EcoSal Plus* Published online December 13, 2016. http://dx.doi.org/10.1128/ecosalplus.ESP-0019-2015
22. Thomas, S. *et al.* (2014) The Type 1 secretion pathway – the hemolysin system and beyond. *Biochim. Biophys. Acta* 1843, 1629–1641
23. Petosa, C. *et al.* (1997) Crystal structure of the anthrax toxin protective antigen. *Nature* 385, 833–838
24. Rigden, D.J. *et al.* (2004) The PA14 domain, a conserved all-β domain in bacterial toxins, enzymes, adhesins and signaling molecules. *Trends Biochem. Sci.* 29, 335–339
25. de Groot, P.W.J. and Klis, F.M. (2008) The conserved PA14 domain of cell wall-associated fungal adhesins governs their glycan-binding specificity. *Mol. Microbiol.* 68, 535–537
26. Maestre-Reyna, M. *et al.* (2012) Structural basis for promiscuity and specificity during *Candida glabrata* invasion of host epithelia. *Proc. Natl. Acad. Sci. U. S. A.* 109, 16864–16869
27. Veelders, M. *et al.* (2010) Structural basis of flocculin-mediated social behavior in yeast. *Proc. Natl. Acad. Sci. U. S. A.* 107, 22511–22516
28. Sim, L. *et al.* (2013) Structural and biochemical characterization of the N-terminal domain of flocculin Lg-Flo1p from *Saccharomyces pastorianus* reveals a unique specificity for phosphorylated mannose. *FEBS J.* 280, 1073–1083
29. Diderrich, R. *et al.* (2015) Structural hot spots determine functional diversity of the *Candida glabrata* epithelial adhesin family. *J. Biol. Chem.* 290, 19597–19613
30. Boyd, C.D. *et al.* (2014) Structural features of the *Pseudomonas fluorescens* biofilm adhesin LapA required for LapG-dependent cleavage, biofilm formation, and cell surface localization. *J. Bacteriol.* 196, 2775–2788
31. Cirillo, S.L.G. *et al.* (2001) *Legionella pneumophila* Entry Gene rtxA Is Involved in Virulence. *Infect. Immun.* 69, 508–517
32. Springer, T.A. (2014) von Willebrand factor, Jedi knight of the bloodstream. *Blood* 124, 1412–1425
33. Barczyk, M. *et al.* (2010) Integrins. *Cell Tissue Res.* 339, 269–280
34. Bienkowska, J. *et al.* (1997) The von Willebrand factor A3 domain does not contain a metal ion-dependent adhesion site motif. *J. Biol. Chem.* 272, 25162–25167
35. Emsley, J. *et al.* (1997) Crystal structure of the I domain from integrin alpha2beta1. *J. Biol. Chem.* 272, 28512–28517
36. Emsley, J. *et al.* (1998) Crystal structure of the von Willebrand Factor A1 domain and implications for the binding of platelet glycoprotein Ib. *J. Biol. Chem.* 273, 10396–10401
37. Lee, J.O. *et al.* (1995) Two conformations of the integrin A-domain (I-domain): a pathway for activation? *Structure* 3, 1333–1340
38. Krishnan, V. *et al.* (2013) Structure of *Streptococcus agalactiae* tip pilin GBS104: a model for GBS pili assembly and host interactions. *Acta Crystallogr. D Biol. Crystallogr.* 69, 1073–1089
39. Emsley, J. *et al.* (2000) Structural basis of collagen recognition by integrin alpha2beta1. *Cell* 101, 47–56
40. Huizinga, E.G. *et al.* (2002) Structures of glycoprotein Ibα and its complex with von Willebrand Factor A1 Domain. *Science* 297, 1176–1179
41. Peyvandi, F. *et al.* (2011) Role of von Willebrand factor in the haemostasis. *Blood Transfus.* 9, s3–s8
42. Schneider, S.W. *et al.* (2007) Shear-induced unfolding triggers adhesion of von Willebrand factor fibers. *Proc. Natl. Acad. Sci. U. S. A.* 104, 7899–7903

43. Ellison, C. and Brun, Y.V. (2015) Mechanosensing: a regulation sensation. *Curr. Biol.* 25, R113–R115
44. Siryaporn, A. *et al.* (2014) Surface attachment induces *Pseudomonas aeruginosa* virulence. *Proc. Natl. Acad. Sci. U. S. A.* 111, 16860–16865
45. Ellison, C.K. *et al.* (2017) Obstruction of pilus retraction stimulates bacterial surface sensing. *Science* 358, 535–538
46. Mignolet, J. *et al.* (2018) More than a Tad: spatiotemporal control of *Caulobacter* pili. *Curr. Opin. Microbiol.* 42, 79–86
47. Wang, Y. and Chen, C. (2005) Mutation analysis of the flp operon in *Actinobacillus actinomycetemcomitans*. *Gene* 351, 61–71
48. Garnham, C.P. *et al.* (2011) Anchored clathrate waters bind antifreeze proteins to ice. *Proc. Natl. Acad. Sci. U. S. A.* 108, 7363–7367
49. Nutt, D.R. and Smith, J.C. (2008) Dual function of the hydration layer around an antifreeze protein revealed by atomistic molecular dynamics simulations. *J. Am. Chem. Soc.* 130, 13066–13073
50. El-Azami-El-Idrissi, M. *et al.* (2003) Interaction of *Bordetella pertussis* adenylate cyclase with CD11b/CD18: Role of toxin acylation and identification of the main integrin interaction domain. *J. Biol. Chem.* 278, 38514–38521
51. Masin, J. *et al.* (2015) *Bordetella* adenylate cyclase toxin: a unique combination of a pore-forming moiety with a cell-invading adenylate cyclase enzyme. *Pathog. Dis.* 73, ftv075
52. Bulutoglu, B. *et al.* (2017) Catch and release: engineered allosterically regulated β-roll peptides enable on/off biomolecular recognition. *ACS Synth. Biol.* 6, 1732–1741
53. Jung, G. *et al.* (2007) Annotation and expression profile analysis of cDNas from the Antarctic diatom *Chaetoceros neogracile*. *J. Microbiol. Biotechnol.* 17, 1330–1337
54. Amin, S.A. *et al.* (2012) Interactions between Diatoms and Bacteria. *Microbiol. Mol. Biol. Rev.* 76, 667–684
55. Croft, M.T. *et al.* (2005) Algae acquire vitamin B12 through a symbiotic relationship with bacteria. *Nature* 438, 90–93
56. Guo, S. *et al.* (2013) Role of Ca^{2+} in folding the tandem β-sandwich extender domains of a bacterial ice-binding adhesin. *FEBS J.* 280, 5919–5932
57. Griessl, M.H. *et al.* (2013) Structural Insight into the giant Ca^{2+}-binding adhesin SiiE: implications for the adhesion of *Salmonella enterica* to polarized epithelial cells. *Structure* 21, 741–752
58. Vance, T.D.R. *et al.* (2014) Ca^{2+}-stabilized adhesin helps an Antarctic bacterium reach out and bind ice. *Biosci. Rep.* 34, e00121
59. Vrielink, A.S.O. *et al.* (2017) Unusually high mechanical stability of bacterial adhesin extender domains having calcium clamps. *PLoS One* 12, e0174682
60. Carrion-Vazquez, M. *et al.* (1999) Mechanical and chemical unfolding of a single protein: a comparison. *Proc. Natl. Acad. Sci. U. S. A.* 96, 3694–3699
61. Li, H. *et al.* (2002) Reverse engineering of the giant muscle protein titin. *Nature* 418, 998–1002
62. Lu, H. *et al.* (1998) Unfolding of titin immunoglobulin domains by steered molecular dynamics simulation. *Biophys. J.* 75, 662–671
63. Oberhauser, A.F. and Carrión-Vázquez, M. (2008) Mechanical biochemistry of proteins one molecule at a time. *J. Biol. Chem.* 283, 6617–6621
64. Luo, Y. *et al.* (2000) Crystal structure of enteropathogenic *Escherichia coli* intimin-receptor complex. *Nature* 405, 1073–1077
65. Wagner, C. *et al.* (2014) The *Salmonella enterica* giant adhesin SiiE binds to polarized epithelial cells in a lectin-like manner. *Cell. Microbiol.* 16, 962–975
66. Gerlach, R.G. *et al.* (2008) Cooperation of *Salmonella* pathogenicity islands 1 and 4 is required to breach epithelial barriers. *Cell. Microbiol.* 10, 2364–2376
67. Wrobel, A. *et al.* (2018) The repeat structure of two paralogous genes, *Yersinia ruckeri* invasin (*yrInv*) and a '*Y. ruckeri* invasin-like molecule', (*yrIlm*) sheds light on the evolution of adhesive capacities of a fish pathogen. *J. Struct. Biol.* 201, 171–183
68. Guo, S. *et al.* (2012) Re-evaluation of a bacterial antifreeze protein as an adhesin with ice-binding activity. *PLoS One* 7, e48805
69. Arahal, D.R. *et al.* (2016) *Marinomonas blandensis* sp. nov., a novel marine gammaproteobacterium. *Int. J. Syst. Evol. Microbiol.* 66, 5544–5549
70. Bai, X. *et al.* (2014) *Marinomonas profundimaris* sp. nov., isolated from deep-sea sediment sample of the Arctic Ocean. *Antonie Van Leeuwenhoek* 106, 449–455
71. Matsunaga, T. *et al.* (2005) Complete genome sequence of the facultative anaerobic magnetotactic bacterium *Magnetospirillum* sp. strain AMB-1. *DNA Res. Int. J. Rapid Publ. Rep. Genes Genomes* 12, 157–166
72. Navarro, M.V.A.S. *et al.* (2011) Structural basis for c-di-GMP-mediated inside-out signaling controlling periplasmic proteolysis. *PLoS Biol.* 9, e1000588
73. Newell, P.D. *et al.* (2009) LapD is a bis-(3′,5′)-cyclic dimeric GMP-binding protein that regulates surface attachment by *Pseudomonas fluorescens* Pf0–1. *Proc. Natl. Acad. Sci. U. S. A.* 106, 3461–3466
74. Koronakis, V. *et al.* (2000) Crystal structure of the bacterial membrane protein TolC central to multidrug efflux and protein export. *Nature* 405, 914–919
75. Koronakis, V. *et al.* (2004) Structure and function of TolC: the bacterial exit duct for proteins and drugs. *Annu. Rev. Biochem.* 73, 467–489
76. Smith, T.J. *et al.* (2018) An N-terminal retention module anchors the giant adhesin LapA of *Pseudomonas fluorescens* at the cell surface: a novel sub-family of type I secretion systems. *J. Bacteriol.* Published online March 26, 2018. http://dx.doi.org/10.1128/JB.00734-17
77. Smith, T.J. *et al.* (2018) Type 1 does the two-step: type 1 secretion substrates with a functional periplasmic intermediate. *J. Bacteriol.* Published online August 24, 2018. http://dx.doi.org/10.1128/JB.00168-18
78. Newell, P.D. *et al.* (2011) A c-di-GMP effector system controls cell adhesion by inside-out signaling and surface protein cleavage. *PLoS Biol.* 9, e1000587
79. Barlag, B. and Hensel, M. (2015) The giant adhesin SiiE of *Salmonella enterica*. *Molecules (Basel, Switzerland)* 20, 1134–1150
80. Borlee, B.R. *et al.* (2010) *Pseudomonas aeruginosa* uses a cyclic-di-GMP-regulated adhesin to reinforce the biofilm extracellular matrix. *Mol. Microbiol.* 75, 827–842
81. Cooley, R.B. *et al.* (2016) Cyclic di-GMP-regulated periplasmic proteolysis of a *Pseudomonas aeruginosa* type Vb secretion system substrate. *J. Bacteriol.* 198, 66–76
82. Kline, K.A. *et al.* (2009) Bacterial adhesins in host–microbe interactions. *Cell Host Microbe* 5, 580–592
83. Krachler, A.M. and Orth, K. (2013) Targeting the bacteria-host interface: strategies in anti-adhesion therapy. *Virulence* 4, 284–294
84. Asadi, A. *et al.* (2018) A review on anti-adhesion therapies of bacterial diseases. *Infection* Published online October 1, 2018. http://dx.doi.org/10.1007/s15010-018-1222-5
85. Ofek, I. *et al.* (2003) Anti-adhesion therapy of bacterial diseases: prospects and problems. *FEMS Immunol. Med. Microbiol.* 38, 181–191
86. Bar Dolev, M. *et al.* (2016) Putting life on ice: bacteria that bind to frozen water. *J. R. Soc. Interface* Published online August 1, 2016. http://dx.doi.org/10.1098/rsif.2016.0210
87. Spaulding, C.N. *et al.* (2017) Selective depletion of uropathogenic *E. coli* from the gut by a FimH antagonist. *Nature* 546, 528–532
88. Spaulding, C.N. *et al.* (2018) Precision antimicrobial therapeutics: the path of least resistance? *Npj Biofilms Microbiomes* 4, 4
89. Guo, S. *et al.* (2018) Conserved structural features anchor biofilm-associated RTX-adhesins to the outer membrane of bacteria. *FEBS J.* 285, 1812–1826